THERMAL BEHAVIOUR OF AMMONIUM MOLYBDATE–BASIC MAGNESIUM CARBONATE SYSTEM DOPED WITH LITHIUM NITRATE

Nagi R. E. Radwan[1]*, Mohammed Mokhtar*[2] *and Gamil A. El-Shobaky*[2*]

[1]Department of Chemistry, Faculty of Education, Suez Canal University, Suez, Egypt
[2]Department of Physical Chemistry, National Research Centre, Dokki, Cairo, Egypt

Abstract

The thermal decomposition of ammonium molybdate–basic magnesium carbonate and the solid–solid interactions of the resulting solids were studied for pure and lithium nitrate doped samples. The techniques employed were TG, DTG, DTA and XRD. The composition of pure calcined solids was $0.5 MoO_3$–MgO and the dopant concentrations were 1, 2 and 4 mol% Li_2O. Pure mixed solids were prepared by wet impregnation method using a known mass of finely powdered basic magnesium carbonate with a calculated amount of ammonium molybdate dissolved in the least amount of distilled water. The three doped samples were prepared by treating basic magnesium carbonate with different proportions of lithium nitrate dissolved in the least amount of distilled water prior to impregnation with ammonium molybdate. The results revealed that lithium doping of the reacting solids enhanced their decomposition and stimulated their solid–solid interaction taking place at ≤500°C yielding $MgMoO_4$ to an extent proportional to its amount added. Opposite effect was observed when the doped solids were heated at >600°C. These results were discussed in terms of an effective increase in the mobility of reacting molybdenum and magnesium species.

Keywords: DTA, Li_2O-doping, MoO_3–MgO system, TG, XRD-techniques

Introduction

Ammonium heptamolybdate, MoO_3 and molybdic acid are widely used for the preparation of supported molybdenum or mixed catalysts [1–5] applied in several reactions such as hydrotreating or partial oxidation [6–9]. Fransen *et al*. [10] have classified the surface structure of molybdena into four different types, namely, solid solution, atomic dispersion, monolayer and particles. Particles or bulk MoO_3 crystals appear with high molybdena loading.

MoO_3 loaded on an active alumina is one of the most important solid catalysts [11–14]. The effects of Li_2O, Na_2O and MgO-doping on solid–solid interaction and phase transformation MoO_3–Al_2O_3 system were investigated using TG, DTG and XRD techniques [15, 16]. It was found that MoO_3 interacts with Al_2O_3 at tempera-

---

tures started at 500°C to produce orthorhombic $Al_2(MoO_4)_3$ and the completion of this reaction requires heating of mixed solids at temperatures above 500°C. The treatment with small amounts of dopant followed by heating at 500°C promoted the solid–solid interaction between Al_2O_3 and MoO_3 to produce aluminum molybdate. The effect of Li_2O-doping was, however, more pronounced than those observed in the case of Na_2O and MgO-doping. The produced aluminum molybdate decomposes at temperatures started from 800°C yielding the corresponding oxides [15, 16]. A portion of MoO_3 sublimed and other portion dissolved in alumina matrix forming MoO_3–α-Al_2O_3 (corundum). It has been found that Al_2O_3 can dissolve 40 mass% MoO_3 [11]. Li_2O-treatment of the MoO_3–Al_2O_3 system decreased the amount of MoO_3 dissolved in the lattice of α-Al_2O_3 (corundum) to an extent proportional to the amount of dopant added [15]. Thermal decomposition of bulk or supported ammonium heptamolybdate in an inert gas atmosphere was studied using different supports [17]. The temperature of heptamolybdate decomposition changes in the sequence: $MgO<unsupported<ZrO_2$, $Al_2O_3<SiO_2<C<Nb_2O_5$. The influence of the support nature on the thermal decomposition of ammonium heptamolybdate in the inert gas was investigated and the properties of different supported oxides were compared.

The present work reports a study on the thermal decomposition of ammonium molybdate supported on MgO and the solid–solid interactions taking place between molybdenum and magnesium substrates as being influenced by Li_2O-treatment. The techniques employed were thermogravimetry (TG), differential thermogravimetry (DTG), differential thermal analysis (DTA) and X-ray diffraction (XRD).

Experimental

Materials

A known mass of basic magnesium carbonate $MgCO_3Mg(OH)_2·2.5H_2O$ (supplied by Fluka Company) was impregnated with ammonium molybdate (supplied by BDH) $(NH_4)_6MoO_7O_{24}·4H_2O$ solutions. The proportion of ammonium molybdate was calculated so that the molar composition of calcined materials was $0.5MoO_3:MgO$. The impregnated materials were dried at 120°C, then calcined at 400, 500, 600, 700, 800 and 900°C. The dried impregnated solids were treated with different proportions of $LiNO_3$ dissolved in the least amount of distilled water prior to calcination at 400–900°C. The time of heating of pure and doped materials was fixed at 5 h. The amounts of lithium were 1, 2 and 4 mol% Li_2O (with respect to the sum of MgO and MoO_3).

Techniques

TG and DTG analyses of various uncalcined materials were carried out using a Perkin Elmer (DT-7 Unix system) thermal analyzer. The reference material was α-Al_2O_3 (corundum). The rate of heating was 10°C min^{-1} and all the measurements were carried out in a current of N_2 flowing at 50 cm^3 min^{-1}.

The X-ray powder diffraction patterns of the various calcined samples were measured using a Philips diffractometer (type P W 1390) with Ni-filtered CuK_α radiation ($\lambda=1.5405$ Å) at 36 kV and 16 mA with a scanning speed of 2° in 2θ min^{-1}.

Results and discussion

Thermal behaviour of pure and doped reacting materials

TG, DTG and DTA curves of pure and variously doped species (ammonium molybdate and basic magnesium carbonate) were determined. Representative thermograms for pure uncalcined mixed solids are given in Fig. 1. Details of the obtained DTA and TG curves for all solids investigated are given in Tables 1 and 2.

Table 1 DTA results for pure and doped materials

Solid	DTA	T_{max}/°C
Pure	endo, vs	232
	endo, s	323
	endo, w	381
	endo, s	433
	endo, s	546
+2 mol% Li_2O	endo, s	180
	endo, w	217
	endo, s	313
	endo, s	398
	endo, s	491
+4 mol% Li_2O	endo, w	115
	endo, w	173
	endo, w	210
	endo, s	300
	endo, s	390
	endo, s	480

w=weak, s=strong, vs=very strong peaks

Several authors [17–20] have studied the mechanisms of the thermal decomposition of ammonium molybdate. The decomposition process took place via the formation of different intermediate compounds, which decompose readily yielding solid MoO_3. The results obtained in the present work suggest the following pathways of the thermal decomposition of the undoped reacting substrates:
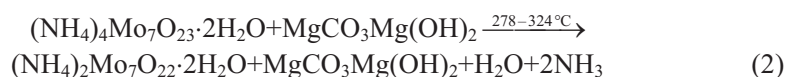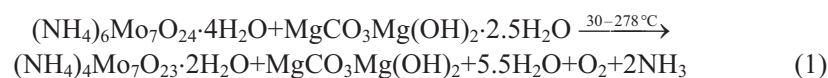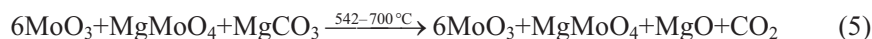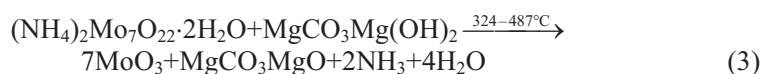
$$(NH_4)_6Mo_7O_{24} \cdot 4H_2O + MgCO_3Mg(OH)_2 \cdot 2.5H_2O \xrightarrow{30-278\,°C}$$
$$(NH_4)_4Mo_7O_{23} \cdot 2H_2O + MgCO_3Mg(OH)_2 + 5.5H_2O + O_2 + 2NH_3 \quad (1)$$

$$(NH_4)_4Mo_7O_{23} \cdot 2H_2O + MgCO_3Mg(OH)_2 \xrightarrow{278-324\,°C}$$
$$(NH_4)_2Mo_7O_{22} \cdot 2H_2O + MgCO_3Mg(OH)_2 + H_2O + 2NH_3 \quad (2)$$

Table 2 TG results of pure and doped materials

Solid	T_{range}/°C	Mass loss/%		Corresponding process
		found	calcd.	
Pure	30–190	1.6		First stage of amm. molybdate decomposition
	190–221	4.8	9.34	
	221–278	3		
	278–324	4.2	4.03	Second stage of amm. molybdate decomposition
	324–377	2.6		Third stage of amm. molybdate decomposition
	377–428	3.6	8.56	
	428–487	2.2		
	487–542	4.6	4.3	Decomposition of uncreacted magnesium carbonate
	542–700	0.5		
+2 mol% Li₂O	30–104	1.2		First stage of amm. molybdate decomposition
	104–156	1.8	9.0	
	156–230	6		
	230–312	5.6	5.6	Second stage of amm. molybdate decomposition
	312–411	9.6	9.6	Third stage of amm. molybdate decomposition
	411–700	4.2	4.2	Decomposition of uncreacted magnesium carbonate
+4 mol% Li₂O	30–88	1.4		First stage of amm. molybdate decomposition
	88–132	2	10.4	
	132–209	7		
	209–260	3.8	8.4	Second stage of amm. molybdate decomposition
	260–300	4.6		
	300–348	2.2	9.8	Third stage of amm. molybdate decomposition
	348–396	7.6		
	396–473	1.4		Decomposition of uncreacted magnesium carbonate
	473–507	2.2	4.0	
	507–700	0.4		

$$(NH_4)_2Mo_7O_{22}\cdot 2H_2O + MgCO_3Mg(OH)_2 \xrightarrow{324-487°C}$$
$$7MoO_3 + MgCO_3MgO + 2NH_3 + 4H_2O \qquad (3)$$

$$7MoO_3 + MgCO_3MgO \xrightarrow{487-542°C} 6MoO_3 + MgMoO_4 + MgCO_3 \qquad (4)$$

$$6MoO_3 + MgMoO_4 + MgCO_3 \xrightarrow{542-700°C} 6MoO_3 + MgMoO_4 + MgO + CO_2 \qquad (5)$$

The first three endothermic peaks in the DTA curves correspond to the formation and decomposition of three intermediate compounds giving rise to MoO_3 and $MgCO_3MgO$ (reactions (1)–(3)). The second set of endothermic peaks correspond to re-
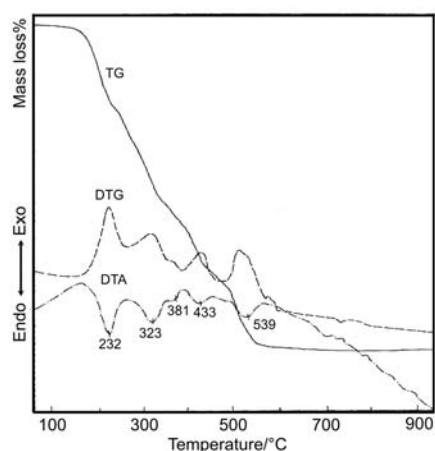
Fig. 1 TG, DTG and DTA curves of uncalcined pure ammonium molybdate–basic magnesium carbonate sample

action (4) giving rise to the formation of $MgMoO_4$ and the last set of endothermic peaks correspond to the complete decomposition of $MgCO_3$ yielding MgO (reaction 5). It has been reported by two of the authors [21] that the thermal decomposition of basic magnesium carbonate yielding MgO takes place at 525.5°C. Inspection of DTA and TG results given in Tables 1 and 2 revealed that Li_2O-treatment enhanced the formation of intermediates and also the solid–solid interactions leading to the formation of $MgMoO_4$. In fact, T_{max} of the first endothermic set of peaks decreased from 232 to 180°C and then 173°C for pure solid samples and those treated with 2 and 4 mol% Li_2O, respectively. Similarly, T_{max} of the second set of endothermic peaks decrease from 323 to 217°C and then 210°C. The T_{max} of the third set of endothermic peaks decreased from 381 to 313°C and then 300°C. The T_{max} of the fourth set of peaks corresponding to the formation of $MgMoO_4$ decreased from 433 to 398°C and then 390°C. The T_{max} of the last set of endothermic peaks corresponding to the complete decomposition of $MgCO_3$ into MgO decreased from 539 to 491°C and then 480°C. The stimulation effect of Li_2O in the formation of intermediate compounds yielding MoO_3 and in solid–solid interactions yielding $MgMoO_4$ and the complete thermal decomposition of $MgCO_3$ can be attributed to the role of lithium ions in increasing the mobility of the reacting species. It has been claimed that the treatment of basic $MgCO_3$ with 6 mol% $LiNO_3$ decreased the decomposition temperature of $MgCO_3$ from 525 to 362°C [21]. The confirmation of the suggested pathways of the reacting substrates could be tested via XRD investigation of the crystalline phases produced at different calcination temperatures.

XRD investigation of pure and variously doped mixed solids precalcined at different temperatures

X-ray diffractograms of pure and doped solids precalcined at temperatures between 400 and 900°C were measured. Inspection of the results revealed that: (i) pure mixed

solids precalcined at 400°C consisted of a mixture of poorly crystalline MgO, MoO_3 and $MgMoO_4$ [22]. The formation of $MgMoO_4$ at 400°C, which is below the decomposition temperature of basic magnesium carbonate yielding MgO suggested that MoO_3 interacted readily with $MgCO_3$ according to:

$$MoO_3 + MgCO_3 \xrightarrow{400\,°C} MgMoO_4 + O_2(g)$$
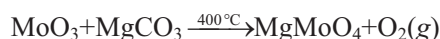
The degree of crystallinity of the produced solids increased by increasing the precalcination temperature from 400 to 500°C. (ii) The Li_2O-treated solids precalcined at 400 and 500°C were composed of a mixture of MgO, MoO_3, $MgMoO_4$ and Li_2MoO_4 having a moderate degree of crystallinity. Figure 2 depicts X-ray diffractograms of pure and doped solids precalcined at 500°C. The comparison between the intensities of the diffraction lines of the phases produced by heating at 500°C showed that Li_2O-doping increased the peak height of the lines of $MgMoO_4$ and MgO and decreased the peak height of MoO_3 (Table 3). These results indicate that Li_2O-treatment enhanced the solid–solid interactions between MgO and MoO_3 yielding $MgMoO_4$ at 400 and 500°C. This treatment led also to an increase in the degree of ordering of MgO as evidenced from the progressive increase in the peak height of the diffraction lines of MgO as a function of the amount of dopant added. The induced increase in the degree of ordering of MgO due to Li_2O-doping might hinder its interaction with MoO_3 to produce $MgMoO_4$. Such an expectation was not verified experimentally since the doping process conduced at 400 and 500°C enhanced magnesium molybdate formation. The stimulation effect of Li_2O towards $MgMoO_4$ formation according to:
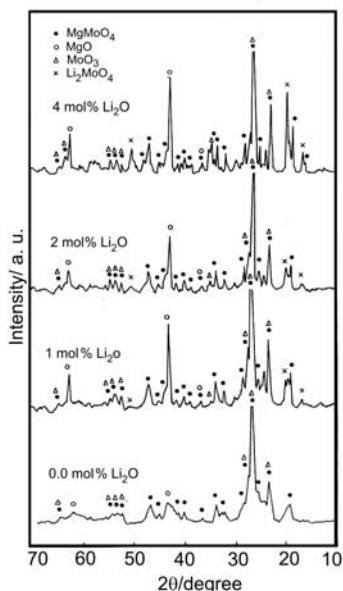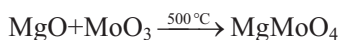
$$MgO + MoO_3 \xrightarrow{500\,°C} MgMoO_4$$

Fig. 2 X-ray diffractograms of pure and various doped $0.5MoO_3$–Mg precalcined at 500°C

could be discussed in terms of an effective increase in the mobility of molybdenum and magnesium species [15].

It has been reported in our previous works that Li_2O-doping increased the mobility of the reacting oxides in MoO_3–Al_2O_3, NiO–Fe_2O_3, Co_3O_4–Fe_2O_3 and MgO–Fe_2O_3 systems [15, 21, 23]. The formation of Li_2MoO_4 in the doped solids precalcined at temperatures starting from 400°C according to:

$$Li_2O + MoO_3 \xrightarrow{400\,°C} Li_2MoO_4$$
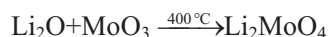
suggested the limited solubility of Li_2O in MoO_3 lattice. These findings point out to the effective role of lithia in increasing the mobility of MoO_3 even when it dissolved a small amount of the dopant in its lattice.

Table 3 The effect of Li_2O-doping on peak height of some diffraction lines of $MgMoO_4$, MgO and MoO_3 phases for the investigated mixed solids precalcined at 500–900°C

Dopant conc./mol%	Calc. temp./°C	$MgMoO_4$/a.u.			MgO/a. u. 2.11 Å	MoO_3/a. u. 3.26 Å
		4.66 Å	3.52 Å	3.16 Å		
0.0		41	54	45	70	115
1.0	500	53	60	60	112	104
2.0		69	60	62	165	91
4.0		92	67	69	190	78
0.0		61	62	54	59	115
2.0	600	43	34	43	72	60
4.0		40	31	30	172	62
0.0		69	65	58	55	
2.0	700	53	45	41	64	(a)
4.0		53	43	40	135	
0.0		94	85	82	83	
1.0	800	66	81	65	142	
2.0		51	77	61	193	–
4.0		51	64	61	227	
0.0		134	146	131	161	
2.0	900	91	106	102	184	–
4.0		41	42	43	228	

(a) The main diffraction line of MoO_3 phase superimposed with the diffraction line of $MgMoO_4$ phase at d-spacing of 3.16 Å

Figures 3 and 4 depict the X-ray diffractograms of pure and variously doped solids precalcined at 700 and 900°C. The effects of Li_2O-doping on solid–solid interactions between MgO and MoO_3 are better investigated by measuring the peak height of some diffraction lines of $MgMoO_4$, MgO and MoO_3. The peak height for the lines located at 4.66, 3.52 and 3.16 Å were considered for $MgMoO_4$; the lines at 2.11 and 3.26 Å were considered for MgO and MoO_3, respectively [22]. The results obtained are given in Table 3 for pure and variously doped solids precalcined at 500, 600, 700, 800 and 900°C. The dif-

fraction lines of Li_2MoO_4 were detected in all doped solids precalcined at 400–900°C which indicates its thermal stability even by heating at 900°C.
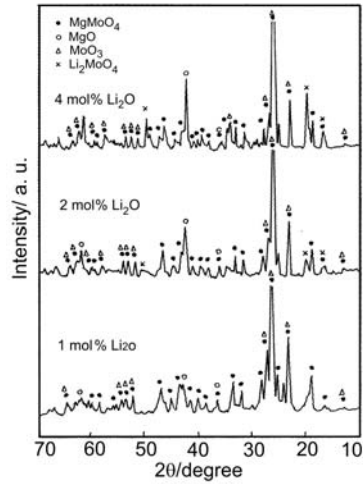

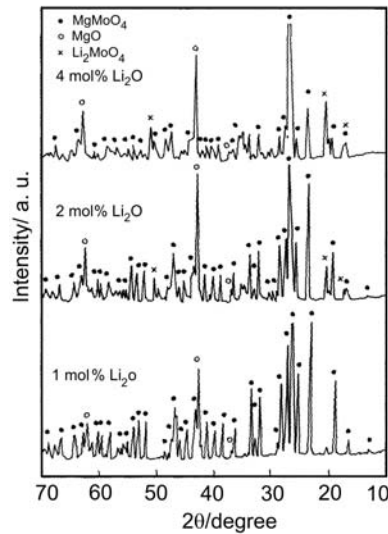**Fig. 3** X-ray diffractograms of pure and variously doped 0.5MoO₃–MgO precalcined at 700°C

Fig. 4 X-ray diffractograms of pure and variously doped 0.5MoO₃–MgO precalcined at 900°C

Inspection of the results given in Table 3 revealed that: (i) The increase in pre-calcination temperature of pure solids in the range of 500–900°C resulted in a progressive increase in the peak height of the diffraction lines of MgMoO₄. This indicates the role of temperature in enhancing the solid–solid interaction between MoO₃ and MgO yielding MgMoO₄. (ii) The peak height of the line at 2.11 Å of MgO [22] changed

slightly upon increasing the calcination temperature from 500 to 800°C then increased suddenly for pure solids precalcined at 900°C. This finding might suggest that the particle size or the degree of crystallinity of MgO, in pure mixed solids, remained almost unchanged by heating in air at 500–800°C then increased by increasing the precalcination temperature to 900°C. (iii) Li_2O-doping followed by calcination at temperatures starting from 600°C resulted in a progressive decrease in the peak height of the diffraction lines of $MgMoO_4$ to an extent proportional to the amount of the dopant added. The decrease in the peak height of the lines of $MgMoO_4$ was, however, more pronounced for the doped solids precalcined at 900°C. (iv) The doping process conducted at 500–900°C brought about a progressive increase in the peak height of the diffraction lines characterizing MgO to an extent proportional to the amount of dopant added. These results suggest that Li_2O-treatment of the investigated solids followed by heat treatment at 600–900°C hindered the solid–solid interaction yielding $MgMoO_4$. The degree of hindrance ran parallel to the amount of the dopant. These results could be discussed in terms of an effective increase in the volatility of MoO_3 as a result of an increase in the mobility of molybdenum ion. In fact, pure MoO_3 melts at 790°C and sublimes by heating in air at ≥800°C [24]. The presence of Li_2O facilitates the melting and the sublimation process of MoO_3 to an extent proportional to its amount present [11, 15]. The enhanced sublimation of MoO_3 due to Li_2O-doping had been reported in the case of MoO_3–Al_2O_3 system [11, 15] subjected to heat treatment at 700–1000°C. It is revealed therefore, that Li_2O-doping of MoO_3–MgO system enhanced the solid–solid interactions taking place at ≥500°C to produce $MgMoO_4$ and hindered these interactions by heating at temperatures above this limit. Both effects could be attributed to an effective increase in the mobility of the reacting oxides.

Conclusions

The following are main conclusions that may be drawn from the obtained results:

1. The Li_2O-doping of ammonium molybdate supported on basic magnesium carbonate with small amount of lithium nitrate enhanced the thermal decomposition of the reacting substrates to an extent proportional to its amount. This enhancement was evidenced from an effective decrease in the temperature of formation of MoO_3 via different intermediate compounds and the decomposition of basic magnesium carbonate.

2. Solid–solid interaction took place between MoO_3 and MgO at temperatures starting from 400°C to produce $MgMoO_4$. The completion of this reaction required the heat treatment at 700°C and the magnesium molybdate formed remained stable up to 900°C.

3. Li_2O-doping enhanced the formation of $MgMoO_4$ taking place at temperatures below 600°C and hindered its formation by heating the reacting solids at temperatures above this limit.

4. Treatment of the reacting solids with Li_2O followed by calcination at 400–900°C brought about a progressive increase in the degree of ordering of MgO.

5. Solid–solid interaction took place between molybdenum and lithium oxides at temperatures starting from 400°C to yield Li_2MoO_4 phase.

References

1 R. Anouchinsky, A. Kaddouri and C. Mazzocchia, J. Thermal Anal., 47 (1996) 299.

2 C. Mazzocchia, A. Kaddouri, R. Anouchinsky, M. Soutel and G. Thomas, J. Thermal Anal., 40 (1993) 1253.

3 A. Roy and J. Ghose, J. Therm. Anal. Cal., 61 (2000) 839.

4 A. Kaddouri, R. DelRosso, C. Mazzocchia and D. Fumagalli, J. Thermal Anal., 36 (2001) 267.

5 M. Kurzawa and M. Bosacka, J. Therm. Anal. Cal., 60 (2001) 177.

6 K. V. R. Charya, T. Bhaskar, J. J. Maheshwar, K. Ramesh and V. V. Rao, Appl. Catal. A, 202 (2000) 133.

7 B. M. Reddya, B. Chowdhurya, E. P. Reddya and A. Fernandez, Appl. Catal. A, 213 (2001) 279.

8 C. Mazzocchia, R. Anouchinsky, A. Kaddouri, M. Sautel and G. Thomas, J. Thermal Anal., 40 (1993) 1253.

9 A. Katrib, P. Leflaive, L. Hilaire and G. Maire, Catal. Lett., 38 (1996) 95.

10 T. Fransen, P. C. Van Berge and P. Mars, Preparation of Catalysts, Elsevier, Amsterdam 1976, p. 405.

11 A. A. Ibrahim and G. A. El-Shobaky, Thermochim. Acta, 147 (1989) 175.

12 Y. Okamato, T. Shimokaws, T. Imanka and S. Teranshi, J. Catal. 57 (1979) 153.

13 P. Gajardo, P. Grang and B. Delmon, Surf. Interface Anal., 3 (1981) 206.

14 R. Margraf, J. Leyrer, H. Knoezinger and E. Taglauer, Surf. Sci., 189–190 (1987) 842.

15 G. A. El-Shobaky, F. H. A. Abdalla, A. M. Ghozza and K. A. Khalil, Thermochim. Acta, 275 (1996) 235.

16 H. G. El-Shobaky, M. Mokhtar and A. S. Ahmed, Thermochim. Acta, 327 (1999) 39.

17 C. Thomazeau, V. Mortin and P. Afnasiev, Appl. Catal. A, 199 (2000) 61.

18 J. C. Valmalette, R. Houriet and H. Hofmann, Eur. J. Solid State Inorg. Chem., 34 (1997) 317.

19 A. A. Said and S. A. Halawy, J. Thermal Anal., 41 (1994) 1075.

20 Yin Zhoulan, Zhao Qinsheng and Chen Shaoyi, J. Cent. - South Inst. Min. Metall, 24 (1993) 541.

21 G. A. El-Shobaky, F. H. A. Abdalla, A. M. Ghozza and K. A. Khalil, Thermochim. Acta, 275 (1996) 235.

22 Powder Diffraction File (JCPDS), international Center for Diffraction Data, Swarthmore, PA 1979.

23 G. A. El-Shobaky, F. H. A. Abdalla and A. M. Ghozza, Thermochim. Acta, 292 (1997) 123.

24 J. G. Grimblot and E. Payen, Surf. Prop. Catal. Non-Metals, 38 (1983) 189.